Journal of Adhesion Science and Technology

ISSN: 0169-4243 (Print) 1568-5616 (Online) Journal homepage: https://www.tandfonline.com/loi/tast20

In depth analysis of anti corrosion behaviour of eco friendly gum exudate for mild steel in sulphuric acid medium

T. Sathiyapriya, G. Rathika & M. Dhandapani

To cite this article: T. Sathiyapriya, G. Rathika & M. Dhandapani (2019): In depth analysis of anti corrosion behaviour of eco friendly gum exudate for mild steel in sulphuric acid medium, Journal of Adhesion Science and Technology, DOI: 10.1080/01694243.2019.1645261

To link to this article: https://doi.org/10.1080/01694243.2019.1645261

Published online: 20 Aug 2019.

JOURNAL OF ADHESION SCIENCE AND TECHNOLOGY
https://doi.org/10.1080/01694243.2019.1645261

In depth analysis of anti corrosion behaviour of eco friendly gum exudate for mild steel in sulphuric acid medium

T. Sathiyapriya[a,b], G. Rathika[a] and M. Dhandapani[c]

[a]Department of Chemistry, PSG College of Arts and Science, Coimbatore, India; [b]Department of Chemistry, Dr. Mahalingam College of Engineering and Technology, Pollachi, India; [c]Post Graduate and Research Department of Chemistry, Sri Ramakrishna Mission Vidyalaya College of Arts and Science, Coimbatore, India

ABSTRACT

The current research work was keen to examine the corrosion inhibition efficiency of mild steel (MS) in presence of aqueous extract of *Araucaria heterophylla* Gum (AHG) in 1 M H_2SO_4 medium. The phytoconstituents of the AHG were interpreted by GC-MS and corrosion inhibition efficiency was deduced using other techniques like weight loss method, potentiodynamic polarization, electrochemical impedance spectroscopy (EIS). Adsorption of inhibitor molecules on the mild steel surface was supported by Density Functional Theory (DFT) studies, Scanning Electron Microscopy (SEM) and Atomic Force Microscopy (AFM). It is seen from the results that the inhibitor exhibits optimum efficiency of 78.57% at 0.05% v/v on mild steel specimen in 1 M H_2SO_4 medium at room temperature. Tafel polarizations clearly show that the aqueous extract of AHG acts as a mixed type inhibitor. The change in the EIS parameters in presence of inhibitor is investigative of the protective layer formation of the mild steel surface. The adsorption is found to obey Langmuir adsorption isotherm. Thermodynamic and activation parameters for the corrosion inhibition process supported the physical adsorption mechanism.

ARTICLE HISTORY
Received 28 February 2019
Revised 12 June 2019
Accepted 9 July 2019

KEYWORDS
GC-MS; Tafel polarization; electrochemical impedance; DFT; surface morphology

1. Introduction

Metal deterioration caused by corrosion is a common phenomenon which occurs due to the interaction of the metals with environmental conditions. Among the several metals mild steel attracted the industries towards itself for its significant economical and substantial uses [1]. In spite of its wide application its usage is restricted because of its limited corrosion resistance in acid media. One of the common methods adopted to avoid the consequences of corrosion is prevention of corrosion by the use of inhibitors. Numerous synthetic inhibitors have been reported as efficient corrosion inhibitor for mild steel, but these are not only expensive but also toxic to both environment and

CONTACT T. Sathiyapriya sathiyachallenge87@gmail.com Department of Chemistry, Dr. Mahalingam College of Arts and Science, Pollachi - 642 003, India

human health [2–4]. The effect of toxicity may be either temporary or permanent and also it may cause either during its preparation or its application.

Hence the present day researchers have been addressed towards the search of low cost, eco-friendly and easily available inhibitors. And thus they used plant products such as extracts of leaves, flowers and gums as corrosion inhibitors for mild steel under different corrosive medium [5–7]. Few of the natural inhibitors of plant origin which have been studied as green eco-friendly inhibitors in acid medium in the the recent past, include *Rubber leaf* [8], *Ginger extract* [9], *Retama monosperma (L.) Boiss. Stems* [10], *Gnetum Africana leaves* [11], *Clerodendrum phlomidis leaves* [12], *Morinda Tinctoria leaves* [13], *Piper longum extract* [14].

Bio polymer form Tragacanth gum and arabinogalactan (AG) was tested as a corrosion inhibitor for carbon steel corrosion in 1 M HCl by Gravimetric method, potentiodynamic polarization measurements, electrochemical impedance spectroscopy, UV–visible spectroscopy, scanning electron microscopy, and atomic force microscopy. At a concentration of 500 ppm at 60 °C, AG produced an inhibition efficiency of 96.3% [15]. In another study, the gum exudates from *Canarium schweinfurthii* was investigated as corrosion inhibitor on mild steel in HCl solution within the temperature range of 303 K to 333 K using gravimetric as well as thermometric techniques. Its efficiency elevated with an elevation in inhibitor concentration, reaching up to 79.10% for mild steel at 303 K at 0.5 g/L concentration [16]. Paul Ocheje Ameh made a comparative study of the inhibitory effect of *Khaya senegalensis* and *Albizia ferruginea* on the corrosion of mild steel in HCl medium. Weight loss methods revealed that both the inhibitors were found to be good corrosion inhibitors for mild steel in acid medium. However, maximum inhibition efficiency was exhibited by *K. senegalensis* with 82.56% inhibition efficiency at 0.5% g/L concentration [17]. Welan Gum and Neem Gum was evaluated as a corrosion inhibitor for steel reinforced in concrete in NaCl media by corrosion characteristic techniques like electrochemical impedance spectroscopy, Tafel polarization study, density functional theory and scanning electron microscopy. The results showed that the two inhibitors inhibited the corrosion of steel in NaCl solution effectively via the formation of protective film [18]. In another study, the gum exudates from *Azadirachta indica* on carbon steel was investigated as corrosion inhibitor on mild steel in 1 N HCl solution using weight loss method, electrochemical studies combined with surface analysis. Its inhibition efficiency increased with increase in inhibitor concentration and shows a maximum efficiency of 77.21% for 323 K at the inhibitor concentration of 100 ppm [19].

There are several research works on polysaccharides as corrosion inhibitors of metals in acid media similar to the ones discussed above, but the assessment on the *Araucaria heterophylla* Gum (AHG) is not known on mild steel corrosion inhibition. AHG has been selected as an environment-friendly corrosion inhibitor for mild steel in 1 M H_2SO_4. The phytoconstituents deduced by GC-MS have shown the presence of multiple bonds and hetero atom and oxygen with lone pair of electrons. The protection of mild steel from aggressive medium has been expected to achieve by the adsorption of the phytoconstituents on to the mild steel surface.

Therefore the current work deals with the investigation of gum exudates from Araucaria heterophylla as corrosion inhibitor for the mild steel in sulphuric acid

medium. The effect of temperature and various other parameters have been studied. Electron density parameters for the phytoconstituents of the AHG and its reactivity indices obtained from density functional theory (DFT) calculations were described. The interest of using AHG as corrosion inhibitor arises because they are safe, eco-friendly and more over water soluble.

2. Materials and methods

2.1. Materials

2.1.1. Preparation of the extract

The AHG was collected from The Queen of hills, Ooty, Tamil nadu, India. The collected AHG samples were washed well with double distilled water to eliminate unwanted dust and other impurities. 1% stock solution was prepared by dissolving exactly weighed 5 g of the AHG in 500 ml of luke warm distilled water.

2.1.2. Preparation of mild steel specimen

Commercially available Mild steel sheets were bought and rectangular mild steel coupons of dimension 2.5 cm × 1 cm × 0.1 cm were prepared. The samples were polished, drilled a hole at one end and numbered by punching. During the study the samples were polished with various grade emery papers, degreased in solution of non-toxic detergent, washed with distilled water and stored in desiccators for further use.

2.1.3. Corrosive medium preparation

Stock solution of 1 M H_2SO_4 was prepared from 97% analar grade supplied by Nice chemicals using double distilled water.

2.2. Methods

2.2.1. GC-MS study

Shimadzu GCMS-QP2010 SE (at PSGCAS, Coimbatore) was utilized to record GC-MS spectrum for AHG extract. Column Elite-1 fused silica capillary column (30 × 0.25 mm ID × 1 µM df, composed of 100% Dimethyl polydiloxane) was employed. The oven temperature was programmed from 100 °C (isothermal for 4 min) to 200 °C at a rate of 10 °C/min and then to 270 °C at a rate of 5 °C/min. Helium was used as a carrier gas at a constant flow of 1 ml/min. An injection volume of 0.5 µl at an injector temperature of 280 °C was employed. Mass spectrum was recorded in electron impact mode at 70 eV, at a scan interval of 0.5 sec and fragments from 40 to 450 Da. Total run time was 53 min.

2.2.2. Mass loss measurements

Weight loss measurements were performed at 303–333 K with different concentrations of AHG extract for 1 hr immersion period. The mild steel plates in triplets were weighed before and after immersion in acid medium. From the weight loss measurements inhibition efficiency (I.E.%), Corrosion rate (CR) and surface coverage (θ) was

calculated using the following Equations (1–3) [20,21]:

$$\text{I.E. } (\%) = \frac{W1 - W2}{W1} \times 100 \tag{1}$$

$$\theta = \frac{W1 - W2}{W1} \tag{2}$$

$$\text{CR} = \frac{534 \times w2}{DAT} \tag{3}$$

where $W1$ and $W2$ are the weight losses (mg) for MS in the absence and presence of AHG inhibitor in acid medium, θ is the surface coverage of the inhibitor molecules, D is Density in g/cm^2 (7.9 g/cm^2 for MS), A is Area of specimen in square inches, T is exposure time in hours. CR is given in miles per year (mpy).

2.2.3. Computational method (DFT studies)

The present quantum chemical calculations were done using Gaussian-09 program of DFT/B3LYP/6-311G (d,p) level of basis set. More than 10 compounds have been isolated in GC-MS analysis, and among them two compounds dihydrotachysterol and Germacrene B and was randomly selected whose peak areas are 8.46 and 5.34 respectively and the computational work was carried out. The correlation between the Inhibition efficiency of the compounds and their electronic properties were clearly studied using this method. Quantum chemical parameters were calculated and the optimized geometric structures for the compounds were drawn by this technique [22,23].

2.2.4. Electrochemical techniques

Electrochemical measurements were taken in a typical three electrode a platinum electrode as a counter electrode, saturated calomel electrode as a reference electrode and mild steel specimen as working electrode at room temperature. The area of the mild steel specimen uncovered to the solution was roughly 1 cm^2. The mild steel specimens were pretreated likewise as done in the gravimetric method. Before each electrochemical measurement, the electrode was allowed to corrode easily and its open circuit potential (OCP) was entered as function of time up to 10 min, which was adequate to become stable. The polarization measurements were taken at a potential range of −200 mV to +200 mV with regard to open circuit potential without and with inhibitor at scan rate of 1 mV/sec. Electrode potentials were measured with respect to standard calomel electrode. The polarization measurements were carried out from a potential range of −200mV to +200mV with respect to open circuit potential in presence and absence of inhibitor at a scan rate of 1 mV/sec.

The EIS measurements were done for mild steel in acid media using Parstat 2273 unit. Corrosion potentials over a frequency range of 0.1 to 20000 Hz with signal amplitude of 10mVwas maintained. From the plot Z' (real) vs Z'' (imaginary), impedance parameters like charge transfer resistance (R_{ct}) and double layer capacitance (C_{dl}) were calculated using the 'EC - Lab' software. The experiments were carried out in 1 M

H_2SO_4 with different inhibitor concentrations. The inhibition efficiency I_{corr} and I.E.% was calculated using the following equations:

$$I_{corr} = \frac{\beta_a \times \beta_c}{2.303\ (\beta_a + \beta_c)} \times \frac{1}{R_{ct}} \tag{4}$$

$$\text{I.E.}(\%) = \frac{I_{corr\ (blank)} - I_{corr\ (inh)}}{I_{corr\ (blank)}} \times 100 \tag{5}$$

$$\text{I.E.}(\%) = \frac{R_{ct\ (blank)} - R_{ct\ (inh)}}{R_{ct\ (blank)}} \times 100 \tag{6}$$

where I_{corr} is corrosion current, R_{ct} is charge transfer resistance, β_a, β_c are Tafel slopes, $I_{corr(blank)}$ is corrosion current without inhibitor, $I_{corr(inh)}$ is corrosion current with inhibitor, $R_{ct(blank)}$ is charge transfer resistance without inhibitor, $R_{ct(inh)}$ is charge transfer resistance with inhibitor.

2.2.5. Surface analysis

2.2.5.1. Scanning electron microscope (SEM). It is a procedure adopted for the analysis of surface morphology of the mild steel sample. The mild steel specimens were dipped in 1 M H_2SO_4 with and without inhibitors for 2 h. The morphology of the mild steel surface in the presence and absence of inhibitors were tested by SEM techniques using FESEM –(SIGMA HV –Carl Zeiss with Bruker Quantax 200 –Z10 EDS Detector).

2.2.5.2. Atomic force microscopy (AFM). The surface morphology of MS coupons were further analysed with the support of AFM (NTEGRA Prima). The test coupons were immersed separately in acid solution without and with 0.05% v/v inhibitor for 1 h at room temperature. After immersion the specimens were taken out, rinsed gently without disturbing the surface and the morphologies were examined.

3. Results and discussion

3.1. Physicochemical properties and plant profile

Physicochemical properties and plant profile is given in Table 1.
Botanical name: Araucaria heterophylla
Family: Araucariaceae
Common name: Christmas tree, Norfolk pine tree, Norfolk Island pine

3.2. GC-MS analysis

3.2.1. Identification of components

Figure 1 shows the GC-MS spectrum of AHG. Interpretation of GC-MS spectrum was done using the database of National Institute Standard and Technology (NIST) having more than 62,000 patterns and NIST library. Thirty peaks were isolated from the GC analysis and Table 2 presents data associated with each of the lines in the spectrum [17,24,25].

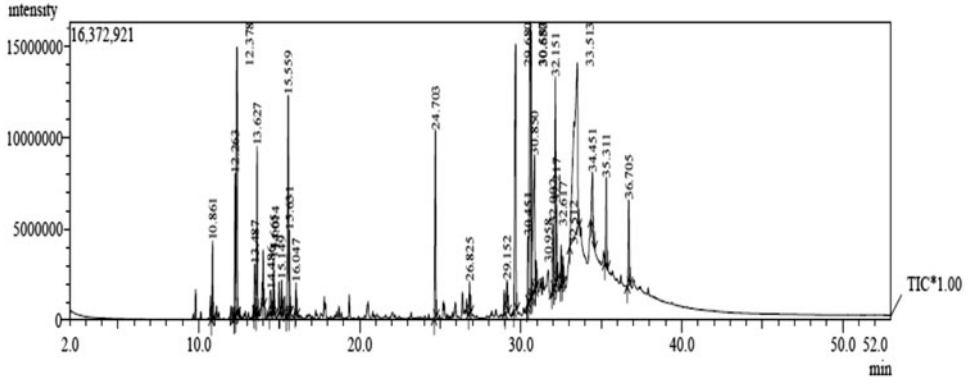

Figure 1. GC-MS spectrum of *Araucaria heterophylla* Gum (AHG).

Table 1. Physicochemical properties of AHG.

Parameters	
pH	Acidic
Colour	Yellowish brown
Odour	
Taste	Non-bitter
Solubility	(a)Cold water: soluble (b)Warm water: soluble (c)Acetone: soluble

Table 2. Phytochemical constituents identified in the acetone extract of AHG using GC-MS.

S.No.	Retention time	Compounds	S.No.	Retention time	Compounds
1.	10.861	Alpha-cubebene	16.	29.68	Dihydrotachysterol
2.	12.263	Gamma-elemene	17.	30.451	Thunbergol
3.	12.378	Cyclo hexane	18.	30.587	Cholest-14-ene
4.	13.487	Naphthalene	19.	30.65	Beta-guaiene
5.	13.627	1,6-cYCLODECADIENE	20.	30.85	Bicyclo[5.3.0]decane
6.	14.014	Bicyclo[8.1.0]undeca-2,6-diene	21.	30.958	Bicyclo[5.3.0]decane
7.	14.486	Isoledene	22.	32.002	Acetic acid
8.	14.665	Beta-cadinene	23.	32.151	9,19-Cycloergost-24(28)-en-3-ol
9.	15.149	Beta-panasinsene	24.	32.217	Betulin
10.	15.559	Germacrene B	25.	32.512	Caryophyllene
11.	15.631	1,6,10-Dodecatrien-3-ol	26.	32.617	Abietic acid
12.	16.047	10,12-Tricosadiynoic acid	27.	3.513	1,3,6,10-Cyclotetradecatetraene
13.	24.703	Phenanthrene	28.	34.451	2-Propenal
14.	26.825	Butanoic acid	29.	35.311	Beta-pimaric acid
15.	29.152	Retinol	30.	36.705	Beta-sitosterol

3.3. Weight loss measurements

Weight loss measurement method was a simple traditional one used to find the weight loss and inhibition potential of the inhibitor [26]. The corrosion rate and inhibition efficiencies for mild steel in the absence and presence of AHG extract for various temperature ranges from 303 to 333 K is given in Table 3. Influence of corrosion rate on temperature at diverse concentrations of the inhibitor in acid medium is displayed in Figure 2. Clear examination of the Table 3 shows that the presence of AHG extract makes the corrosion rate to decrease in all the studied temperature and at all inhibitor

Table 3. CR and IE (%) of AHG extract in 1 M H_2SO_4 at different concentrations and different temperatures.

		303 K		313 K		323 K		333 K	
S. no.	Inhibitor conc. % (v/v)	CR (mpy)	I.E. (%)	CR (mpy)	I.E. (%)	CR (mpy)	I.E. (%)	CR (mpy)	I.E. (%)
1.	Blank	0.3223	-	1.3123	-	2.5325	-	5.4563	-
2.	0.003	0.2763	14.286	0.9439	28.07	2.0720	18.18	4.812	11.81
3.	0.009	0.1842	42.86	0.7367	43.86	1.7497	30.91	4.674	14.35
4.	0.015	0.1151	64.29	0.4604	64.91	1.4734	41.82	4.259	21.94
5.	0.020	0.0691	78.57	0.3453	73.68	0.9669	61.82	2.532	53.59
6.	0.050	0.0691	78.57	0.3223	75.44	0.8979	64.55	2.325	57.38

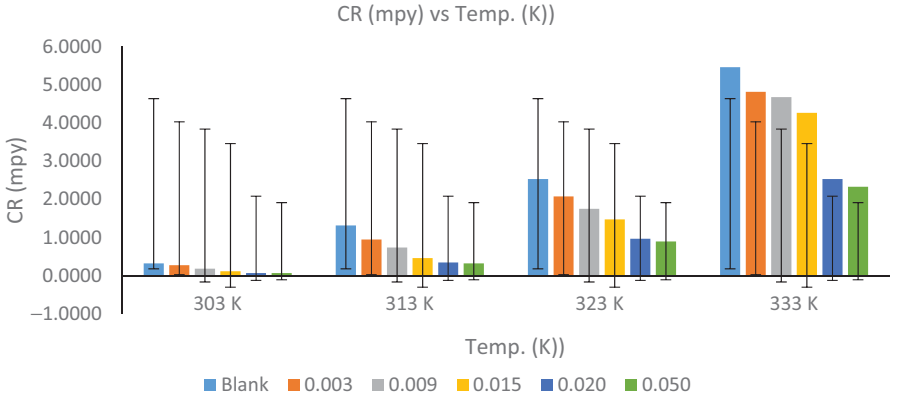

Figure 2. Influence of corrosion rate on temperature at different concentrations of AHG extract in 1 M H_2SO_4 medium.

concentrations. It is noticed that the I.E.% increases on increasing the concentration of the inhibitor for all temperatures. Increase in I.E.%, i.e., the inhibitive effect is attributed to the fact that the phytochemical constituents containing oxygen present in the AHG extract gets adsorbed on the mild steel surface. Thus adsorbed inhibitor molecules act as a barrier and protects the metal from corrosion [27]. It is also seen that the I.E.% decreases from 78.57 to 57.38% in the corrosive medium and hence the maximum inhibition efficiency is attained at303 K with 0.05% v/v of inhibitor concentration. The decrease of I.E.% with increasing temperature indicates the metal dissolution at higher temperatures. A general rule says that the rate of the reaction increases with increase in the temperature, which leads to the formation of activated molecules. This is why the reactant molecules gain more energy, and overcome the energy barrier more quickly. And also the increased temperature dissolves the protective layer on the metal surface, thus makes the metal susceptible to corrosion [28]. Decreased inhibition efficiency with the increase in temperature is suggestive of the physisorption mechanism [29].

3.4. Activation parameters

3.4.1. Activation energy (E_a)

Activation energy is the important parameter which states the type of adsorption process. A plot of log CR vs 1/T (shown in Figure 3) was made and from the slope of the plot E_a

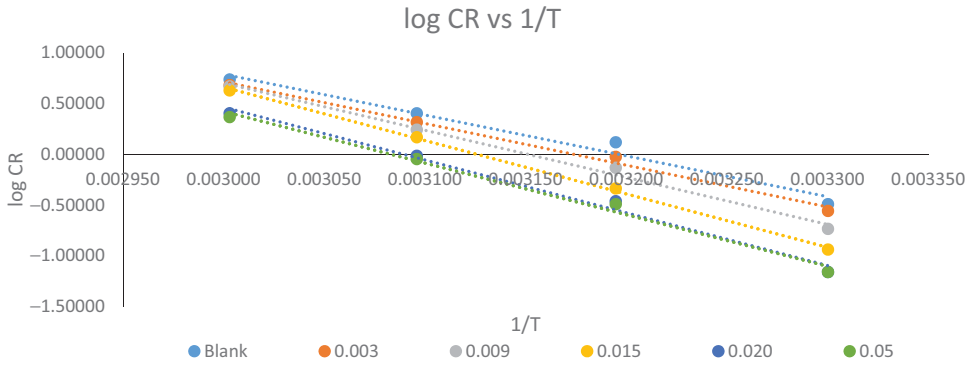

Figure 3. Arrhenius plot.

Table 4. Activation parameters of 1 M H_2SO_4 mild steel surface in both uninhibited and inhibited solutions.

S.No.	Inhibitor conc. (% v/v)	$-Ea$ (KJ mol^{-1})	$-\Delta H^*$(KJ mol^{-1})	ΔS^*(J mol^{-1})
1.	Blank	77.019	74.38	11.52
2.	0.003	78.679	76.04	15.07
3.	0.009	88.818	86.18	45.21
4.	0.015	100.762	98.12	80.31
5.	0.02	99.586	96.95	72.99
6.	0.05	97.363	94.72	65.52

values for the mild steel specimen in the presence and absence of various concentrations of the AHG extracts were calculated.

Thus elucidated E_a values according to the Equation (5) were exhibited in Table 4:

$$\mathrm{CR} = K\mathrm{e}^{Ea/RT} \tag{7}$$

Where CR is the corrosion rate, E_a is activation energy, T is the absolute temperature, K is the Arrhenius pre exponential constant and R is the gas constant. From the concept of collision theory it is said that the acid molecules corrodes the metal surface, by means for collision between the acid and the metal surface. Thus sulphuric acid molecules secure higher energy in the presence of inhibitor for the corrosion reaction to occur; by the way corrosion inhibition takes place [30]. On further examination of the data in Table 4 it is found that the E_a values are high for inhibited acid solutions than for the uninhibited acid medium. This type of behaviour is suggestive of the formation of a protective film on the surface of the mild steel which supports physical adsorption type mechanism [31].

3.4.2. Enthalpy and entropy of activation (ΔH^* and ΔS^*)

The enthalpy of activation (ΔH^*) and entropy of activation (ΔS^*) are the two components which are obtained from the temperature dependence of a rate constant of a reaction. These can be obtained from the slope and intercept of transition state plot of log (CR/T) against 1/T. The enthalphy of activation (ΔH^*) and entropy of activation

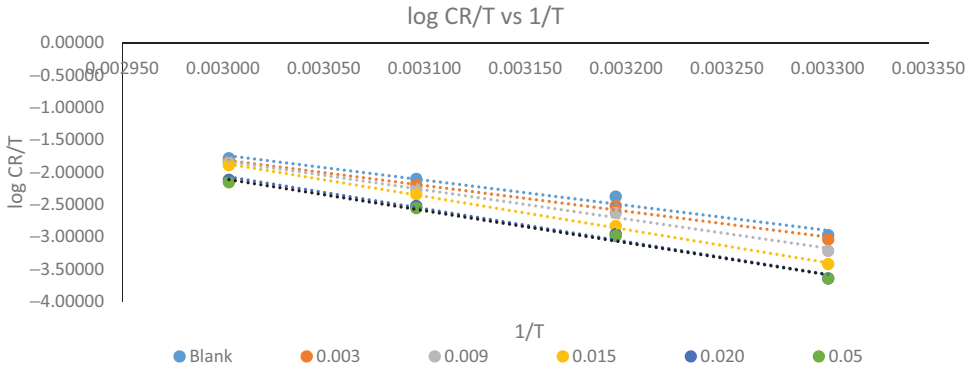

Figure 4. Transition state plot.

(ΔS^*) are calculated using the Eyring equation (Equation (7)).

$$\mathrm{CR} = (RT/Nh)\ \exp^{\Delta S*/R} \mathrm{e}^{-\Delta H*/RT} \tag{8}$$

where R is the gas constant, T is the absolute temperature, N is the Avagadro number, h is the Planck's constant. The linear plot with a slope of ($\Delta H^*/R$) and an intercept of ($\log(R/Nh) + \Delta S^*/R$) are obtained as shown in the Figure 4.

The ΔS^* provides ideas about the type of molecularity of the rate determining step in a corrosion reaction. It is seen from the Table 4 the positive values of ΔS^* shows that the entropy increases upon addition of inhibitor, which often indicates a dissociative mechanism in which the activated complex is loosely bound and about to dissociate [32]. Likewise negative values of ΔH^* for both the inhibited and the uninhibited solutions in the sulphuric acid medium which reflects the adsorption of inhibitor molecules on the mild steel inhibition process is exothermic [33].

3.5. Thermodynamic and adsorption studies

The fundamental information about the type of interaction among the mild steel and the inhibitor molecules can be provided by the adsorption isotherm. Attempts were made to fit surface coverage θ) values to different adsorption isotherms, among that the best fit was obtained by Langmuir adsorption isotherm. The R^2 values which found close to unity is an indicative factor for the strong adherence of the adsorption of the inhibitor molecules on the surface of the mild steel. Figure 5 Shows the Langmuir adsorption isotherm for the adsorption of the inhibitor molecules on the mild steel [34,35].

Langmuir adsorption equation is given by Equation (9):

$$\frac{C}{\Theta} = \frac{1}{K_{ads}} + C \tag{9}$$

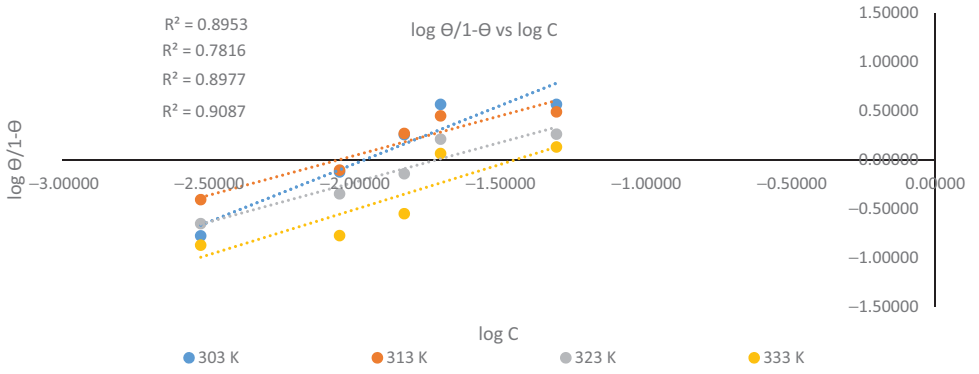

Figure 5. Langmuir adsorption isotherm.

Table 5. Values of free energy for the adsorption of AHG extract in 1 M H_2SO_4 on the mild steel surface at different temperature.

		$-\Delta G_{ads}$ KJ mol^{-1}			
S.No.	Inhibitor Conc. % (v/v)	303 K	313 K	323 K	333 K
1.	0.003	20.22	23.10	22.32	21.61
2.	0.009	21.24	22.05	21.25	19.19
3.	0.015	22.16	22.96	21.15	19.21
4.	0.02	23.23	23.29	22.56	22.32
5.	0.05	20.92	21.15	20.42	20.21

Where Θ is the surface coverage, K_{ads} is adsorption equilibrium constant, C is the inhibitor concentration.

$$\Delta G_{ads} = \quad -2.303\,RT\log\left(55.5K\right) \tag{10}$$

Free energy values are calculated using the Equation (10) and are presented in Table 5. The negative free energy values are less than the threshold value of –40 kJ/mol. And thus the adsorption of AHG on mild steel surface supports the physisorption mechanism [36].

3.6. Electrochemical measurements

3.6.1. Potentiodynamic polarization

Figure 6 shows the potentiodynamic polarization curves of mild steel in 1 M H2SO4 absence and presence of different concentrations of AHG extract. The kinetic parameters like corrosion potential (E_{corr}), Corrosion current density (I_{corr}), anodic Tafel slopes ($ß_a$), cathodic Tafel slopes ($ß_c$), Polarization resistance (R_p) and I.E. (%) are presented in Table 6. On investigating the data in the Table. 6 it is seen that there prevails an inverse relationship between I_{corr} and R_p, on increasing the concentration of the inhibitor. On observation of the data in the Table 6 the I_{corr} of mild steel decreases on increasing the concentration of the inhibitor, which proves the inhibiting nature of aqueous extract of AHG. Whereas the E_{corr} values and the Tafel slopes do not form a specific tendency which indicates that the process of metal corrosion inhibition in the acid medium follows mixed type. In all concentrations $ß_c$ is greater than $ß_a$ suggesting

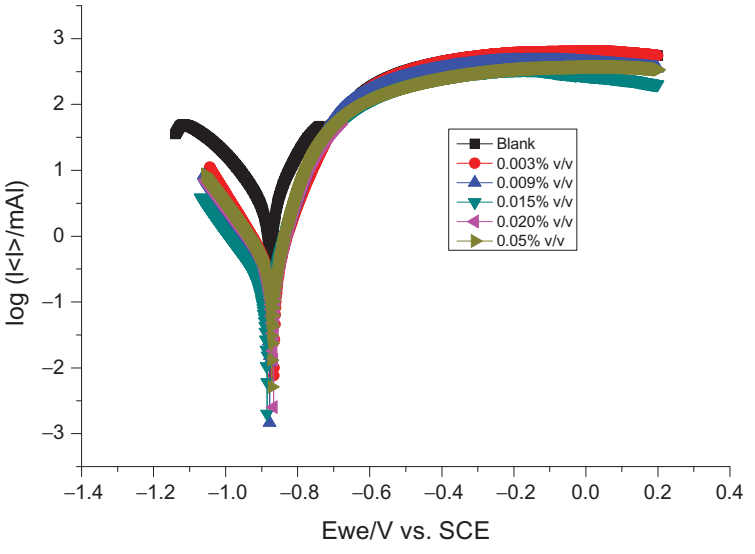

Figure 6. Potentiodynamic polarization curves for mild steel in 1 M H_2SO_4 containing different concentrations of the inhibitor (AHG).

Table 6. Kinetic parameters of mild steel in 1 M H_2SO_4containing different concentrations of the inhibitor.

							IE (%)	
S.No.	Inhibitor conc. (% v/v)	$-E_{corr}$ (mV)	I_{corr} (μA)	$ß_a$ (mV/dec)	$ß_c$ (mV/dec)	R_p (Ω cm^2)	I_{corr}	R_p
1	Blank	874.84	3727.79	112.5	189.3	82.19	**	**
2	0.003	868.22	308.28	71.2	112.8	614.79	91.73	86.63
3	0.009	879.36	231.5	65	116.3	782.08	93.79	89.49
4	0.015	885.54	153.17	61.3	132.3	1187.56	95.89	93.08
5	0.02	866.30	285.87	60.7	135	636.02	92.33	87.08
6	0.05	872.00	362.42	62.5	133.1	509.55	90.28	83.87

that though the inhibition is under mixed control, the effect of the inhibitor on the cathodic polarization is more pronounced than on the anodic polarization [13]. The R_p values determined using I_{corr} values showed a gradual increase on increasing the concentration of the inhibitor. The I.E. (%) calculated for I_{corr} and R_p values are found increasing on increased concentration of the inhibitor.

3.6.2. Impedance measurements

The Nyquist plots obtained for mild steel in1 M H_2SO_4 and 1 M H_3PO_4 solutions with various concentrations of AHG extracts are shown in Figure 7. Electrochemical parameters like charge transfer resistance (R_{ct}) related to the OCP corrosion reaction, while the CPE represents a constant phase element related to the non-ideal capacity (Double layer capacitance (C_{dl})) for different inhibitor concentrations in the corrosive medium are presented in Table 7. Clear inspection of the data in Table 7 proves that the R_{ct} values increase with increased inhibitor concentration. The R_{ct} value increases from 4.346 to 53.291 Ω for maximum concentration of the AHG (0.05% (v/v)) in 1 M H_2SO_4.

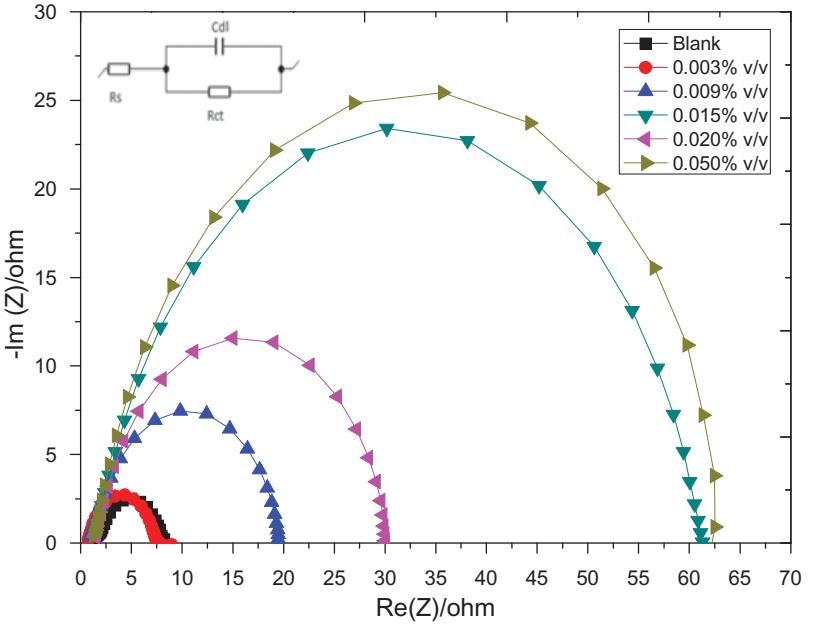

Figure 7. Nyquist plot of mild steel in 1 M H_2SO_4 in the absence and presence of various concentration of inhibitor (AHG).

Table 7. Impedance parameters for mild steel in 1 M H_2SO_4 and 1 M H_3PO_4 in the absence and presence of various concentrations of inhibitor.

						IE%	
S. No.	Inhibitor conc. (% v/v)	R_{ct} (Ω cm^2)	R_s (Ω cm^2)	n	C_{dl} (μF cm^{-2})	C_{dl}	R_{ct}
1	Blank	4.346	1.94	362.4	35900		-
2	0.003	5.599	1.71	68.5	109300	69.55	22.38
3	0.009	6.065	1.54	60.2	624200	82.61	28.34
4	0.015	25.295	1.38	55.1	605000	83.15	82.82
5	0.02	52.966	1.22	50.5	385100	89.27	91.79
6	0.05	53.291	1.18	46.2	454600	87.34	91.84

The increase in the thickness of the electrical double layer is proved from the decrease in the C_{dl} values [37].

3.7. Quantum chemical approach

3.7.1. Frontier molecular orbital (FMO) calculations

E_{HOMO}, is the energy of the highest occupied molecular orbital indicates the electron donation by the molecule which signifies the better donation of electron and facilitate the adsorption of the inhibitor molecules and possess good inhibition efficiency. E_{LUMO}, is the energy of the lowest unoccupied molecular orbital measures the electron accepting nature of the molecule. E_{HOMO}, E_{LUMO} and optimized geometric images for the investigated compounds are given in Figure 8(a,b).

Upon analysing Table 8, it is clear that the E_{HOMO} value for the four studied compounds follow the order as compound (A) > (B) which shows that compound (A) has the highest electron donating ability among the other compounds. The energy gap

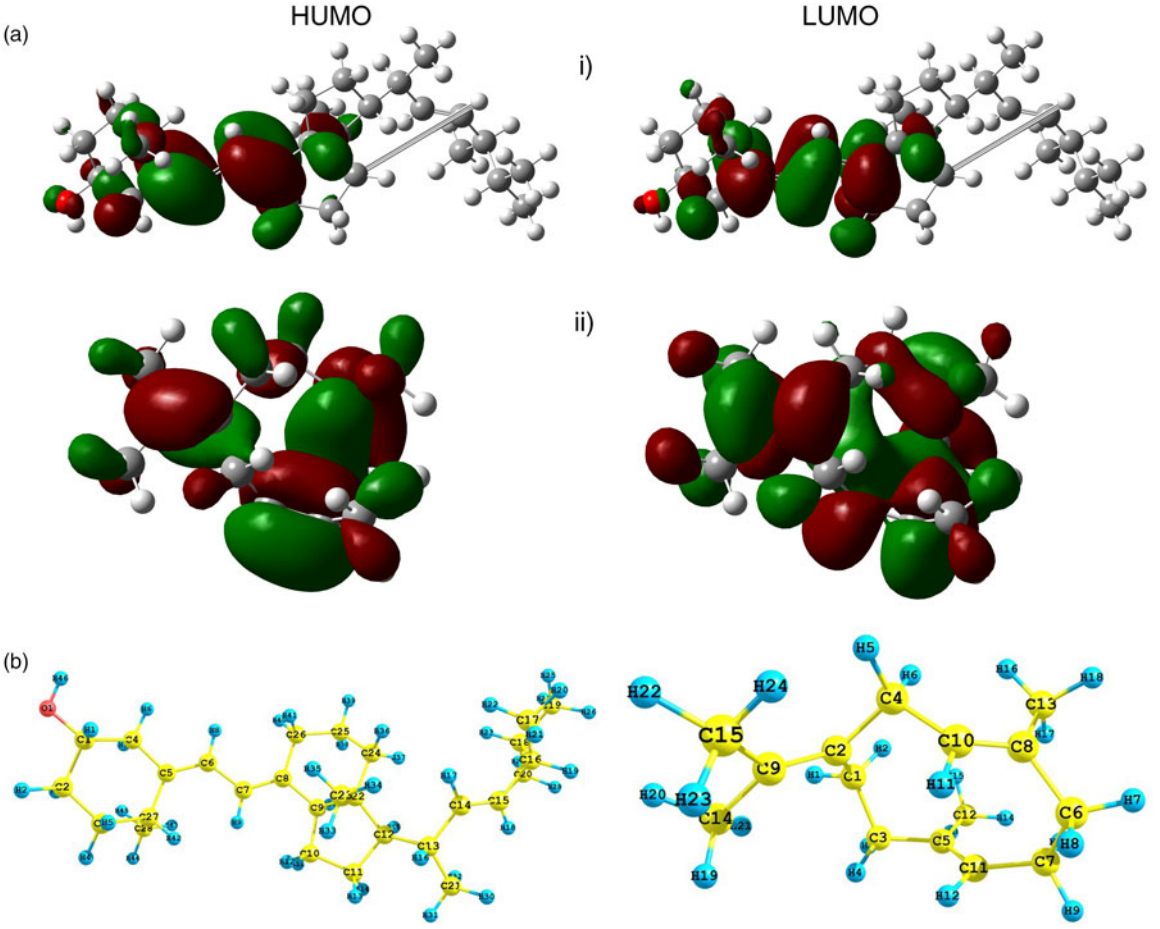

Figure 8. (a) E_{HOMO} and E_{LUMO} images of (i) Dihydrotachysterol (compound A) (ii) Germacrene B (compound B). (b) Optimised structures of (i) Dihydrotachysterol (compound A) (ii) Germacrene B.

Table 8. Quantum chemical parameters for the compounds studied.

S.No.	Quantum descriptor	Dihydrotachysterol (compound A)	Germacrene B (compound B)
1.	E_{HOMO} (eV)	−5.3207	−5.60314
2.	E_{LUMO} (eV)	−0.368	0.26612
3.	Energy gap (ΔE) (eV)	4.9527	5.8692
4.	Dipole moment (μ)	1.7533	0.2919
5.	Ionization energy (I)	5.3207	5.60314
6.	Global hardness (η)	2.4764	2.93468
7.	Global softness (S)	0.40382	0.34075
8.	Fraction of electrons transferred (Δn)	0.83907	0.73799
9.	$\Delta E_{Back\ -Donation}$ (eV)	−0.6191	−0.73367
10.	Electrophilicity index (ω)	1.63352	1.2133
11.	Chemical potential	−2.8444	−2.66851

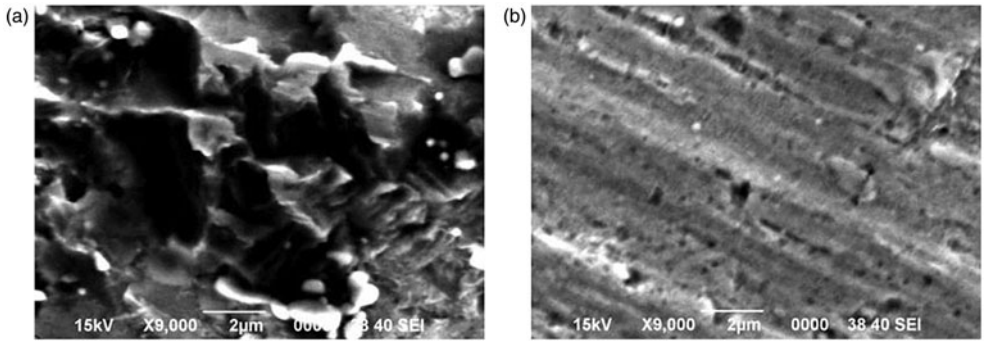

Figure 9. (a,b) Corrosion surface morphology.

between the E_{HOMO} and E_{LUMO} renders information about the reactivity of the inhibitor towards the surface of the mild steel. There exist a perfect relation between the energy gap ΔE and the inhibition efficiency that is decrease in the ΔE increases the reactivity of the inhibitor molecules which in turn increases the inhibition efficiency. So for the compound to deliver better I.E.%, the energy gap should be low, since the energy needed to remove the electron form the last occupied orbital will be less. The results as shown in Table 8 indicate that the compound (A) possess the lowest ΔE value, which means that the compound could have render better inhibition than the other compound. Dipole moment is a DFT parameter which explains about the nature of adsorption of the inhibitor on the mild steel. Many researchers have reported that higher the dipole moment more will be the inhibition efficiency. In that manner compound (A) exhibits a higher μ as 1.7533 which supports its inhibition efficiency. Ionization energy is an important parameter which deals with the chemical reactivity of the atoms and molecules. It is an important factor that higher the ionization energy, stability and the chemical inertness of the compound will be high, whereas a low ionization energy provides high reactivity of the atoms and molecules. In that feature, compound (C) possesses low ionization energy of 5.3207 eV but gives high I.E.% in comparison to other compounds (A), (B) and (D). Global reactivity descriptors, hardness and softness are measures of stability and reactivity. It is said that compound having low global hardness and high softness is likely to give enhance inhibition efficiency.

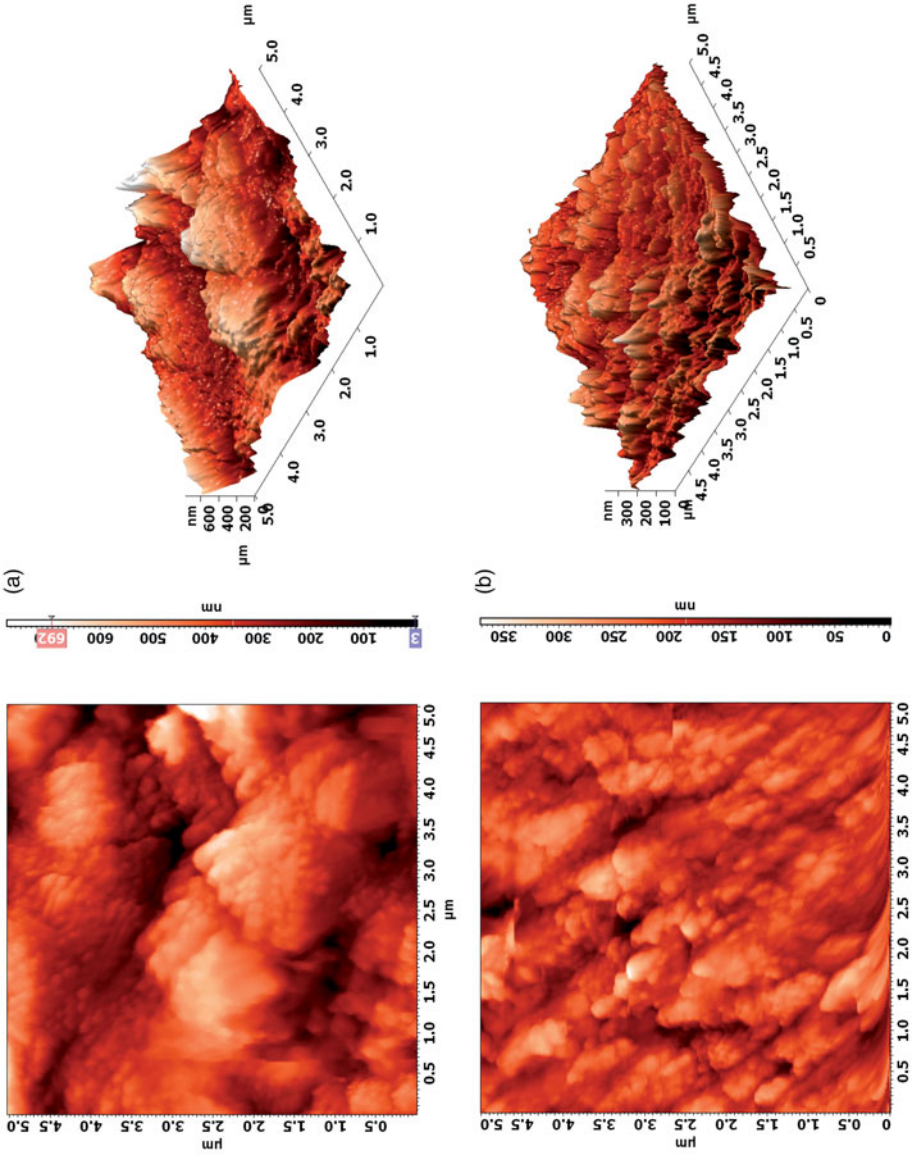

Figure 10. AFM images of mild steel in 1 M H_2SO_4 after 2 h immersion time. (a) Mild steel specimen without inhibitor. (b) Mild steel specimen with optimum concentration of the AHG inhibitor.

In that aspect compound (C) possesses a lower global hardness as 2.4764 eV and a higher softness value as 0.40382 eV compared with other compounds. The fraction of electrons transferred (Δn) and back donation of electrons ($\Delta E_{\text{Back - Donation}}$ (ev)) was determined and shown in Table 8. According to Lukovits study, increase in electron donating capability of the inhibitor molecule to donate electrons to the mild steel surface increases the inhibition efficiency. Among the two compounds studied, compound (A) has a higher value of Δn indicating a higher inhibition efficiency [38–42].

3.8. Surface morphology

3.8.1. SEM analysis

Figure 9(a,b) presents image of the SEM images of mild steel immersed in 1 M H_2SO_4 in presence and absence of aqueous extract of AHG after 2 h immersion period. It is seen that the mild steel plate corroded aggressively in the blank acid medium which is shown in Figure 9(a,b) shows the photograph of smoother surface of mild steel specimen, which is recognized to the fact that the inhibitor forms a protective film on the surface of the mild steel [43].

3.8.2. Atomic force microscopy (AFM)

Figure 10(a,b) represents the AFM images of mild steel in the absence and presence of AHG after immersion of 2 h. It is seen from the images that the mild steel was highly damaged in the absence of inhibitor and the roughness (Sa) calculated is 87.278 nm whereas the value is 30.229 nm for mild steel dipped in acid medium containing AHG inhibitor. The decrease in the values strongly supports the adsorption of inhibitor molecules on the surface of the mild steel surface [44].

4. Conclusions

The natural Gum exudate of the plant is found to be an effective corrosion inhibitor for mild steel in 1 M H_2SO_4 medium and the experimental results concluded that the inhibition efficiency was concentration and temperature dependent. The phytoconstituents present in the AHG get adsorbed on the mild steel surface followed Langmuir adsorption isotherm. The values of E_a and the ΔG confirm the physisorption and spontaneity of the corrosion process respectively. EIS revealed the charge transfer and Tafel polarization indicated that the AGH acts as mixed type inhibitor. SEM, EDX and AFM techniques supported the inhibition process well.

Disclosure statement

No potential conflict of interest was reported by the authors.

ORCID

M. Dhandapani http://orcid.org/0000-0003-4233-6779

References

[1] Chigondo M, Chigondo F. Recent natural corrosion inhibitors for mild steel: an overview. J Chem. 2016;2016:1–7.

[2] Bhawsar J, Jain PK, Jain P. Experimental and computational studies of *Nicotiana tabacum* leaves extract as green corrosion inhibitor for mild steel in acidic medium. Alexandria Eng J. 2015;54:769–775.

[3] Li X, Deng S, Fu H. Inhibition of the corrosion of steel in HCl, H_2SO_4 solutions by bamboo leaf extract. Corros Sci. 2012;62:163–175.

[4] Sathishkumar P, Kumaravelan V, Dhivyapriya D. Comparative study of mild steel corrosion using hydrochloric acid and phosphoric acid medium with ocimum tenuiflorum (l) plant extract. Int J Advanced Res. 2015;3:643–651.

[5] Dakeshwar Kumar Verma KF. Corrosion inhibition of mild steel by extract of *Bryophyllum pinnatum* leaves in acidic solution. Chem Mat Res. 2015;7:69–76.

[6] Dehghani A, Bahlakeh G, Ramezanzadeh B. A detailed electrochemical/theoretical exploration of the aqueous *Chinese gooseberry* fruit shell extract as a green and cheap corrosion inhibitor for mild steel in acidic solution. J Mol Liq. 2019;282:366–384.

[7] Satapathy AK, Gunasekaran G, Sahoo SC. Corrosion inhibition by *Justicia gendarussa* plant extract in hydrochloric acid solution. Corros Sci. 2009;51:2848–2856.

[8] Okewale AO, Olaitan A. The use of rubber leaf extract as a corrosion inhibitor for mild steel in acidic solution. Int J Mat Chem. 2017;7:5–13.

[9] Fidrusli A S, Mahmood M. Ginger extract as green corrosion inhibitor of mild steel in hydrochloric acid solution. IOP Conf. Series: Mat Sci Eng. 2018;290:012087.

[10] Fdil R, Tourabi M, Derhali S, et al. Evaluation of alkaloids extract of *Retama monosperma* (L.) Boiss. stems as a green corrosion inhibitor for carbon steel in pickling acidic medium by means of gravimetric, AC impedance and surface studies. J Mater Env Sci. 2018;9:358–369.

[11] Nnanna LA, Owate IO, Nwadiuko OC, et al. Adsorption and corrosion inhibition on *Gnetum africana* leaves extract on carbon steel. Int J Mat Chem. 2013;3:10–16.

[12] Pruthviraj RD, Prakash CH., Somasheklariah Mild steel corrosion inhibition by plant extract in 0.1 M Hydrochloric acid solution. Scholars J Eng Technol. 2013;1:169–171.

[13] Krishnaveni K, Ravichandran J, Selvaraj A. Effect of *Morinda tinctoria* leaves extract on the corrosion inhibition of mild steel in acid medium. Acta Metall Sin. 2013;26: 321–327.

[14] Singh A, Ahamad I, Quraishi MA. *Piper longum* extract as green corrosion inhibitor for aluminium in NaOH solution. Arab J Chem. 2016;9:S1584–S1589.

[15] Mobin M, Rizvi M, Olasunkanmi LO, et al. Biopolymer from Tragacanth gum as a green corrosion inhibitor for carbon steel in 1M HCl solution. ACS Omega. 2017;2: 3997–4008.

[16] Ameh PO. Electrochemical and computational study of gum exudates from *Canarium schweinfurthii* as green corrosion inhibitor for mild steel in HCl solution. J Taibah Univ Sci. 2018;12:783–795.

[17] Ameh PO. A comparative study of the inhibitory effect of gum exudates from *Khaya senegalensis* and *Albizia ferruginea* on the corrosion of mild steel in hydrochloric acid medium. Int J Metals. 2015;2015:13.

[18] Annaamalai MGL, Maheswaran G, Ramesh N, et al. Investigation of corrosion inhibition of Welan Gum and Neem Gum on reinforcing steel embedded in concrete. Int J Electrochem Sci. 2018;13:9981–9998.

[19] Malarvizhi M, Mallika J. Efficacy of corrosion inhibitive properties of gum exudate of *Azadirachta indica* on carbon steel in 1N Hydrochloric acid. Orient J Chem. 2018;34: 2487–2494.

[20] Ansari K, Quraishi MA, Singh A. Chromenopyridin derivatives as environmentally benign corrosion inhibitors for N80 steel in 15% HCl. J Assoc Arab Univ Basic Appl Sci. 2017;22:45–54.

[21] Sathiyapriya T, Rathika G. Corrosion inhibition efficiency of bio-waste on mild steel in acid media. Orient J Chem. 2015;31:1703–1710.
[22] Chaitra TK, Mohana KN, Gurudatt DM, et al. Inhibition activity of new thiazole hydrazones towards mild steel corrosion in acid media by thermodynamic, electrochemical and quantum chemical methods. J Taiwan Inst Chem Eng. 2016;67:521–531.
[23] Frisch MJ, Trucks GW, Schlegel HB, et al. Gaussian 09 [webpage]. Revision E.01. Wallingford CT: Gaussian Inc.; 2009.
[24] Eddy NO, Odiongenyi AO, Ameh PO, et al. Corrosion inhibition potential of *Daniella oliverri* gum exudates for mild steel in acidic medium. Int J Electrochem Sci. 2012;7: 7425–7439.
[25] Eddy NO, Ameh P, Gimba CE, et al. GCMS Studies on *Anogessus leocarpus* (Al) gum and their corrosion inhibition potential for mild steel in 0.1 M HCl. Int J Electrochem Sci. 2011;6:5815–5829.
[26] Sheeja VN. Inhibition Effect of Environmentally Benign - Grewia tiliaefolia, Pavetta indica and Schleichera oleosa Bark and Leaves Extract on Corrosion of Mild Steelin Acid Media. Coimbatore (TN): Avinashilingam University for Women; 2015.
[27] Asadi N, Ramezanzadeh M, Bahlakeh G, et al. Utilizing lemon balm extract as an effective green corrosion inhibitor for mild steel in 1M HCl solution: A detailed experimental, molecular dynamics, Monte Carlo and quantum mechanics study. J Taiwan Inst Chem Eng. 2019;95:252–272.
[28] Dehghani A, Bahlakeh G, Ramezanzadeh B, et al. Potential of Borage flower aqueous extract as an environmentally sustainable corrosion inhibitor for acid corrosion of mild steel: electrochemical and theoretical studies. J Mol Liq. 2019;277:895–911.
[29] Dasami PM, Parameswari K, Chitra S. Inhibition of mild steel corrosion in 1M H_2SO_4 medium by benzimidazole mannich bases. Orient J Chem. 2015;31:185–191.
[30] Ituen EB, James AO, Akarana O. Fluvoxamine-based corrosion inhibitors for J55 steel in aggressive oil and gas well treatment fluids. Egyptian J Chem. 2017;26:745–756.
[31] Al-Amiery AA, Kadhum AAH, Mohamad AB. Electrochemical study on newly synthesized chlorocurcumin as an inhibitor for mild steel corrosion in hydrochloric acid. Mat. 2013;6:5466–5477.
[32] Aejitha S, Kasthuri PK, Geethamani P. Comparative study of corrosion inhibition of *Commiphora caudata* and *Digera muricata* for mild Steel in 1M HCl solution. Asian J Chem. 2016;28:307–311.
[33] Goyal M, Yadav O, Kumar R, et al. Experimental, surface characterization and computational evaluation of the acid corrosion inhibition of mild steel by methoxycarbonyl methyl triphenyl phosphonium bromide (MCMTPPB). Indian J Chem Technol. 2017; 24:256–268.
[34] Dada AO, Olalekan AP, Olatunya AM, et al. Langmuir, Freundlich, Temkin and Dubinin–Radushkevich isotherms studies of equilibrium sorption of Zn^{2+} unto phosphoric acid modified rice husk. J Applied Chem. 2012;3:38–45.
[35] Shukla SK, Ebenso EE. Corrosion inhibition, adsorption behavior and thermodynamic properties of streptomycin on mild steel in hydrochloric acid medium. Inter J Electro Sci. 2011;6:3277–3291.
[36] Brindha T, Revathi P, Mallika J. Corrosion inhibition of naturally occurring gum exudates of *Araucaria columnaris* on mild steel in 1M H_2SO_4. Int J Environmental Sci. 2015;4:36–43.
[37] Khaled KF. Electrochemical behavior of nickel in nitric acid and its corrosion inhibition using some thiosemicarbazone derivatives. Electrochim Acta. 2010;55:5375–5383.
[38] Kouakou V, Niamien PM, Yapo AJ, et al. Experimental and DFT studies on the behavior of caffeine as effective corrosion inhibitor of copper in 1M HNO_3. Orbital: Electron J Chem. 2016;8:66–79.
[39] Dehghani A, Bahlakeh G, Ramezanzadeh B, et al. A combined experimental and theoretical study of green corrosion inhibition of mild steel in HCl solution by aqueous *Citrullus lanatus* fruit (CLF) extract. J Mol Liq. 2019;279:603–624.

[40] Saxena A, Prasad D, Haldhar R, et al. Use of Saraca ashoka extract as corrosion inhibitor for mild steel in 0.5M H2SO4. J Mol Liq. 2018;58:89–97.
[41] John S, Joseph A, Sajini T, et al. Corrosion inhibition properties of 1,2,4-hetrocyclic systems: electrochemical, theoretical and Monte Carlo simulation studies. Egypt J Pet. 2017;26:721–732.
[42] Kowsari E, Arman SY, Shahini MH, et al. *In situ* synthesis, electrochemical and quantum chemical analysis of an amino acid-derived ionic liquid inhibitor for corrosion protection of mild steel in 1M HCl solution. Corrosion Sci. 2016;112:73–85.
[43] Ameer MA, Fekry AM. Corrosion inhibition of mild steel by natural product compound. Progr Org Coat. 2011;71:343–349.
[44] Verma C, Quraishi MA. 2-Amino-4-(2,4-dihydroxyphenyl) quinoline-3-carbonitrile as sustainable corrosion inhibitor for SAE 1006 steel in 1 M HCl: electrochemical and surface investigation. J Assoc Arab Univ Basic Appl Sci. 2017;23:29–36.